Original Research

Translational and Rotational Forces on Heart Valve Prostheses Subjected Ex Vivo to a 4.7-T MR System

Maria-Benedicta Edwards, MPhil,[1]* Roger J. Ordidge, PhD,[2] David L. Thomas, PhD,[2] Jeffrey W. Hand, PhD,[3] and Kenneth M. Taylor, MD,[1]

Purpose: To assess the magnetic field interactions on 60 heart valve prostheses subjected to a 4.7 T MR system. It addresses the question of whether heart valves deemed safe at 1.5 T may pose safety hazards as patients are exposed to increased static magnetic fields.

Materials and Methods: Ex vivo testing was performed to evaluate translational and rotational forces on 60 heart valves using previously described techniques.

Results: Translational forces were detected on 58 heart valves ranging from 0.5° to 7.5°. Seven valves exhibited paramagnetic/weakly ferromagnetic behavior, and 51 valves exhibited diamagnetic behavior. Rotational forces were observed for 46 valves.

Conclusions: Criteria previously used for safety assessment of heart valve prostheses and expressed in terms of magnetic forces suggest the forces observed in this study are compatible with the safe use of these valves in magnetic resonance (MR) systems with static fields up to 4.7 T.

Key Words: heart valves; magnetic resonance imaging; translational and rotational forces; MRI safety; implants
J. Magn. Reson. Imaging 2002;16:653–659.

THE USE OF MAGNETIC RESONANCE (MR) imaging has become commonplace in clinical practice despite its relatively short history. Anxieties persist, however, about the interaction between the magnetic field and biomedical implants and devices and how this can affect the patient. Potentially dangerous magnetic field interactions can occur when ferromagnetic materials are exposed to the static magnetic field. The resultant translational (attraction or deflection) and rotational (torque) forces may lead to the dislodgement of the implant and/or its malfunction (1–6), or to a device becoming a projectile (7,8), both of which may result in injuries to the patient and/or MR personnel, as well as damage to the device.

Numerous studies have been conducted to evaluate the safety criteria for exposing patients with biomedical implants and devices to MR systems and procedures. Results indicate that few biomedical implants are absolutely contraindicated for MR imaging (2–6). Patients who have received many types of implants, including metallic ones, are considered safe to undergo a MR procedure, as long as the implanted device is non-ferromagnetic or, if the magnetic attraction of the implant is much less than the forces applied in its in vivo application (9–15). Safety and compatibility of devices implanted in patients exposed to a MR system must take into consideration the potential for injury to the patient, damage to or impairment of function of the device, and/or its impact as a potential source of image artifacts. Studies to date have focused mainly on MR systems with strengths of 1.5 T or less; however, higher field strength MR systems are being developed, and there are currently approximately 50 3- to 4-T MR systems in operational use at research and clinical institutions (3,16–20).

Higher B_0 field strength MR systems have the potential to enhance the clinical use of MR imaging, MR spectroscopy, and functional MR imaging. However, patients will potentially be exposed to increased static magnetic fields, and, as a likely consequence, larger time varying fields. Implants currently deemed safe in a 1.5-T field, may, for example, pose significant safety hazards at higher field strengths (18,20–22). It is therefore important to test biomedical implants and devices at higher field strengths than has been done hitherto to identify and assess magnetic field interactions and to identify the potential hazards for patients and personnel. In this study, we assessed the magnetic field-induced forces on 60 different heart valve prostheses exposed ex vivo to a 4.7-T MR system.

[1]United Kingdom Heart Valve Registry, Department of Cardiothoracic Surgery, Hammersmith Hospital, London, UK.
[2]Department of Medical Physics, University College London, London, UK.
[3]Radiological Sciences Unit, Hammersmith Hospital, London, UK.
This work has neither been presented at an ISMRM meeting nor has it been accepted for presentation at a future meeting.
*Address reprint requests to: M.B.E., United Kingdom Heart Valve Registry, Department of Cardiothoracic Surgery, Hammersmith Hospital, Du Cane Road, London W12 0NN UK. E-mail: m.b.edwards@ic.ac.uk
Received February 20, 2002; Accepted July 24, 2002.
DOI 10.1002/jmri.10201
Published online in Wiley InterScience (www.interscience.wiley.com).

Table 1
List of Heart Valves Evaluated for Safety at 4.7 T*

No.	Valve name	Valve type	Site	Model	Size (mm)	Cage and occluder	Sewing ring
1	ATS Medical Open Pivot Valve	Mechanical bileaflet	Mitral	500 FA	25	Pyrolitic carbon, titanium	Velour Dacron®, Teflon
2	Beall	Mechanical caged disc	Mitral	Unknown[a]	29	Pyrolitic carbon	Pyrolitic carbon with Dacron®
3	Biocor	Porcine bioprosthesis	Aortic	H3636	23	Porcine, Celcon	Dacron®
4	Bjork Shiley 60°cc	Mechanical tilting disc	Aortic	ABC	27	Pyrolitic carbon, chromium cobalt alloy	Teflon
5	Bjork Shiley 60°cc Valve Graft	Mechanical valve graft	Aortic	AGVCM	25	Pyrolitic carbon, chromium cobalt alloy	Teflon
6	Bjork Shiley Conical Disc	Mechanical tilting disc	Mitral	MBUP	21	Pyrolitic carbon, chromium cobalt alloy	Teflon
7	Bjork Shiley Conical Disc	Mechanical tilting disc	Mitral	MBRP	21	Pyrolitic carbon, chromium cobalt alloy	Teflon
8	Bjork Shiley Spherical Disc	Mechanical tilting disc	Mitral	MBP	31	Pyrolitic carbon, chromium cobalt alloy	Teflon
9	Bjork Shiley Monostrut	Mechanical single leaflet	Aortic	ABMS	17	Pyrolitic carbon, chromium cobalt alloy	Teflon
10	Bjork Shiley Monostrut	Mechanical single leaflet	Mitral	MBUM	25	Pyrolitic carbon, chromium cobalt alloy	Teflon
11	Bjork Shiley Monostrut	Mechanical single leaflet	Mitral	MBRMS	23	Pyrolitic carbon, chromium cobalt alloy	Teflon
12	Bjork Shiley Monostrut	Mechanical single leaflet	Mitral	Unknown	33	Pyrolitic carbon, chromium cobalt alloy	Teflon
13	Carbomedics (standard)	Mechanical bileaflet	Aortic	500	21	Pyrolitic carbon, titanium,	Dacron® coated with Biolite
14	Carbomedics Supra-annular (Top Hat)	Mechanical bileaflet	Aortic	S500	23	Pyrolitic carbon, titanium	Dacron® coated with Biolite
15	Carbomedics (standard)	Mechanical bileaflet	Mitral	700	31	Pyrolitic carbon, titanium	Dacron® coated with Biolite
16	Carbomedics SuMit	Mechanical bileaflet	Mitral	S700	29	Pyrolitic carbon, titanium	Dacron® coated with Biolite
17	Carbomedics Valve Graft	Mechanical bileaflet valve graft	Aortic	AP500	34	Graphite, pyrolite, titanium	Dacron® + gelweave graft
18	Carpentier Edwards	Porcine bioprosthesis	Aortic	2625	31	Porcine xenograft, flexible Elgiloy® (cobalt nickel alloy) frame	Tubular knitted porous Teflon
19	Carpentier Edwards Pericardial	Pericardial bioprosthesis	Mitral	6900	33	Bovine pericardium, Elgiloy®, (cobalt nickel alloy) frame	Polyester & silicone
20	Carpentier Edwards Supra-annular	Porcine bioprosthesis	Mitral	6650	31	Porcine xenograft, Elgiloy®, PTE cloth	Silicone rubber with PTFE cloth
21	Durafic	Human tissue	Aortic	AD	33	Dura mater	Unknown
22	Durafic	Human tissue	Mitral	MD	23	Dura mater	Unknown
23	Duromedics	Mechanical bileaflet	Aortic	3160	27	Pyrolitic carbon, stellite	Dacron® coated with Biolite
24	Duromedics	Mechanical bileaflet	Mitral	9210	29	Pyrolitic carbon, stellite	Dacron® coated with Biolite
25	Hancock Pericardial	Pericardial bioprosthesis	Mitral	T410	25	Bovine pericardium, polypropylene	Haynes alloy with polyester fibre
26	Hancock Modified Orifice	Porcine bioprosthesis	Aortic	250	21	Porcine xenograft, Dacron® with Haynes alloys #25, polypropylene flexible stent with Stellite	Dacron® with silicone rubber
27	Hancock Modified Orifice II	Porcine bioprosthesis	Aortic	T505	25	Porcine xenograft, acetal homopolymer covered with polyester fabric	Haynes alloys #25 with polyester fabric
28	Intact	Porcine bioprosthesis	Aortic	A805	19	Porcine pericardium, acetyl copolymer covered with Dacron®	Polyester fabric
29	Intact	Porcine bioprosthesis	Mitral	M705	25	Porcine pericardium, acetyl copolymer covered with Dacron®	Polyester fabric
30	Ionescu Shiley	Pericardial bioprosthesis	Aortic	ISA	23	Bovine pericardium, titanium covered with Dacron®	Teflon
31	Jyros	Mechanical bileaflet	Aortic	JA1	26	Pyrolitic carbon impregnated with Boron Carbide, carbon	Warp knitted polyester
32	Jyros	Mechanical bileaflet	Mitral	JIM	30	Pyrolitic carbon impregnated with Boron Carbide, carbon	Warp knitted polyester
33	Labcor Synergy ST	Porcine bioprosthesis	Aortic	TLPB-A	21	Porcine pericardium composite, copolymer	Silicone
34	Labcor Synergy ST	Porcine bioprosthesis	Mitral	TLPB-M	25	Porcine pericardium composite, copolymer	Silicone
35	Liotta	Porcine bioprosthesis	Aortic	MA783	23	Porcine, acetalic resin frame (Delrin) low profile stent with Dacron ® cloth	Dacron®
36	Medtronic Hall	Mechanical single leaflet	Aortic	A7700	23	Pyrolitic carbon with graphite substrate titanium	Teflon

37	Medtronic Hall	Mechanical single leaflet	Mitral	M7700	23	Pyrolitic carbon with graphite substrate titanium	Teflon
38	Medtronic Hall	Mechanical single leaflet	Mitral	MHK	29	Pyrolitic carbon with graphite substrate titanium	Teflon
39	Mira	Mechanical bileaflet	Mitral	9600	27	Pyrolitic carbon, Carbofilm® coated titanium alloy	Knitted polyester cloth
40	Mitroflow	Porcine bioprosthesis	Aortic	11A	25	Bovine pericardium, acetal homopolymer, medical grade polyester	Flexible tungsten loaded silicone
41	Mitroflow	Porcine bioprosthesis	Aortic	141	25	Bovine pericardium, Delrin® 500, Dacron fabric	Flexible tungsten loaded silicone
42	Mitroflow	Porcine bioprosthesis	Mitral	121	29	Bovine pericardium, Delrin® 500, Dacron fabric	Flexible tungsten loaded silicone
43	Mitroflow Synergy	Porcine bioprosthesis	Aortic	12A	21	Bovine pericardium, acetal homopolymer, medical grade polyester	Flexible tungsten loaded medical Grade silicone
44	Mosaic	Porcine bioprosthesis	Aortic	305	29	Porcine xenograft, acetal homopolymer	Polyester fabric
45	Omniscience	Mechanical single leaflet	Mitral	2522	25	Pyrolitic carbon, titanium (nickel free)	Polyester (Dacron)
46	On-X	Mechanical bileaflet	Aortic	ONXA	19	ON-X™ pyrolitic carbon	PTFE
47	On-X	Mechanical bileaflet	Mitral	ONXM	31–33	ON-X™ pyrolitic carbon	PTFE
48	Smellof Cutter	Mechanical caged ball	Aortic	SA	21	Silicone rubber, titanium with bar metal	Polyester and Teflon
49	Sorin Pericarbon (stented)	Pericardial bioprosthesis	Mitral	SM	33	Bovine pericardium, polyacetal resin + tantalum wire	PET Carbofilm™ coated
50	St Jude Mechanical	Mechanical bileaflet	Aortic	AEC	21	Pyrolitic carbon	Double velour Dacron® cloth
51	St Jude Mechanical	Mechanical bileaflet	Mitral	MEC	27	Pyrolitic carbon	Double velour Dacron® cloth
52	Starr Edwards	Mechanical caged ball	Mitral	6120	32	Silicone rubber, barium sulphate, Stellite alloy #21	Porous knitted Teflon + polypropylene cloth
53	Starr Edwards	Mechanical caged ball	Mitral	6320	32	Stellite alloy #21, cloth interrupted with metal studs, polypropylene over Teflon	Knitted Teflon + polypropylene
54	Starr Edwards	Mechanical caged disc	Mitral	6520	26	Polyethylene & titanium, Stellite alloy #21 + polypropylene	Knitted Teflon + polypropylene
55	Tascon	Porcine bioprosthesis	Aortic	300	23	Porcine xenograft, Elgiloy®	Polyester
56	Ultracor	Mechanical single leaflet	Aortic	3800	23	Pyrolitic carbon, grade A-70 titanium	Knitted Teflon
57	Ultracor	Mechanical single leaflet	Mitral	4800	25	Pyrolitic carbon, grade A-70 titanium	Knitted Teflon
58	Wessex	Porcine bioprosthesis	Aortic	WAX10	31	Porcine xenograft, acetal copolymer	Cloth reinforced silicone rubber
59	Wessex	Porcine bioprosthesis	Mitral	WMV20	25	Porcine xenograft, acetal copolymer	Cloth reinforced silicone rubber
60	Xenofic	Porcine bioprosthesis	Aortic	AP80	23	Bovine pericardium	Teflon with stainless steal marker

Manufacturers listed by valve numbers: Alliance Medical, Wakefield, UK (9–12); Aortech Europe Ltd. Strathclyde, UK (56, 57); ATS Medical Inc., Minneapolis, MN, USA (1); Axion Medical, West Sussex, UK (31, 32); Coratomic Inc., Indianapolis, IN, USA (2); Cutter Laboratories, Irvine, CA, USA (48); Edwards Lifesciences, Irvine, CA, USA (18–20, 23, 24, 39, 52–54); Heart Institute, Sao Paolo, Brazil (21, 22); Implantes Medicos S.A., Madrid, Spain, South America (60); Medical Incorporated Inc., Austin, TX, USA (45); Medtronic Inc., Minneapolis, MN, USA (25–29, 36–38, 44, 55); Mitroflow International Inc., Austin, TX, USA (41, 42); Pulse Surgical Ltd., Oxon, UK (46, 47); Shiley Inc., Irvine, CA, USA (4–8, 30); Sorin Biomedica Cardio SpA, Saluggia, Italy (49, 58, 59); St. Jude Medical Inc., St. Paul, MN, USA (3, 35, 50, 51); Sulzer Carbomedics UK Ltd., West Sussex, UK (13–17, 33, 34, 40, 43).

[a]Unknown. The authors were unable to identify the details of the model from the explanted valve.

MATERIALS AND METHODS

Heart Valve Prostheses

Sixty heart valve prostheses were investigated and evaluated for MR safety. The study included many widely implanted heart valves (23), 35 of which were mechanical and 25 were either bioprostheses or valves made from human tissue. Full details of the individual heart valve prostheses are shown in Table 1.

4.7-T MR System

A 4.7-T super-conducting passively shielded MR system (Magnex, Oxford) with a clear bore of 90 cm and 220-ton iron shield was used in the investigation. To relate the forces exerted on the heart valve prostheses to the static magnetic field gradient of the MR system, the gradients were measured using a Bell 640 Incremental Gauss Meter and axial probe. The highest magnetic gradient measured was 5 T/m and occurred at a distance of 40 cm from the portal of the MR system (approximately 95 cm from the magnet center).

Assessment of Magnetic Field Interactions

A standard technique was used to assess interactions between the magnetic field and biomedical implants and devices (4,10,24). The forces giving rise to deflection and rotation on each of the 60 heart valve prostheses were assessed using the non-ferromagnetic test rig shown in Figure 1. The test rig was placed parallel to the magnetic field and the deflection angle test was conducted at the position inside the shielded 4.7-T MR system where the spatial gradient of the magnetic field was determined to be at a maximum. Each heart valve was suspended at its estimated center by a piece of light-weight thread 30 cm long. A mirror was positioned at 45° to a protractor to allow the investigators to accurately read and record the angle of deflection. To avoid parallax error, the protractor was etched on opaque glass. The accuracy of the measuring device was ± 0.2°. Each heart valve was returned to the vertical position twice, and two investigators confirmed the angle of deflection for both measurements.

The translational force exerted on materials with susceptibility $\chi \ll 1$ is given by:

$$F_{trans} = \frac{\chi^V}{\mu_o} B_o \frac{\partial B}{\partial z} \quad (1)$$

where V is the volume of the material and the only significant component of the magnetic field gradient ∇B is assumed to be $\partial B/\partial z$ (i.e., $\partial B/\partial z > \partial B/\partial x$ or $\partial B/\partial y$). The relationship between F_{trans} and θ, the observed angle of deflection of the prosthesis is

$$F = mg\ sin\theta \quad (2)$$

where m is the mass of the prosthesis and g is the acceleration due to gravity (9.81 meters/second^2). The sense of deflection is dependent upon whether the prosthesis is diamagnetic (negative χ) or paramagnetic (positive χ) (25).

Further assessment of magnetic field interactions was conducted to determine the presence of magnetic field-induced torque. Each heart valve was placed both parallel and perpendicular to the magnetic field near the center of the MR system, where the field was homogenous and had been measured at its maximum (4.7 T), in order to observe any movement in terms of rotation or alignment to the magnetic field. Each valve was suspended vertically by a lightweight thread attached to the sewing ring and suspended from the test rig outside the MR system in such a way that its orientation was parallel (180°) or perpendicular (90°) to the long axis of the bore (Fig. 2). The rig was then carefully moved into the center of the MR system taking care not to change the orientation of the suspension system. Two observations were taken for each position and the following three-point qualitative scale of measurement was applied; 0 = zero torque; +1 = alignment or rotation of > 0° to 45° from the starting position; +2 = alignment or rotation of > 45° to 90° from the starting position.

Magnetic moments were calculated for the individual prostheses because they enable the forces on them to be estimated in any magnet once the field gradients present have been measured. In addition, the force exerted upon each of the heart valves exposed to the 4.7-T MR system that experienced a deflection was calculated in order to compare this with the force of the naturally beating heart to determine whether a field of 4.7 T has the potential to dislodge or move the valve in situ.

RESULTS

Table 2 presents the test results for 60 different heart valve prostheses evaluated for magnetic field interactions arising from a 4.7-T MR system. Only two valves showed zero interaction with the magnetic field, both in terms of deflection and torque. All the other heart valves demonstrated some measure of interaction. Deflection angles for 59 of the heart valves ranged from 0° to 7.5°. It was not possible to obtain an angle of deflection for one valve, the Carbomedics Valve Graft1, due to the length of the root graft interfering with the freedom of movement of the valve.

Within the mechanical group of valves, only four displayed a zero deflection; all other valves deflected by between 0.5° and 7.5°. The bioprosthetic and human tissue valves displayed deflections between 0° and 7°, with the majority of valves deflecting by 2°. The higher deflections recorded were seen in all the valve groups. Seven valves were attracted towards the center and highest field, indicating they were slightly paramagnetic/weakly ferromagnetic. All other valves deflected away from the center of the magnet, corresponding to diamagnetic behavior (Table 2).

Only 12 of the 60 heart valves did not align or rotate towards the magnetic field. When placed parallel to the magnetic field, 15 valve prostheses gave measurements

[1]This valve had been loaned to the study for evaluation. Therefore, the investigators were unable to trim the root graft for the purposes of the study.

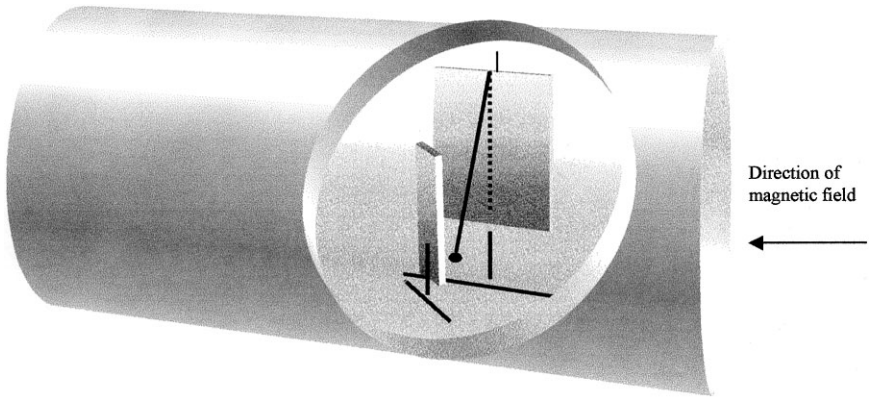

Figure 1. Diagram of the 4.7-T MR system and device used to measure translation and rotational forces on prosthetic heart valves (side view).

of +1, i.e., aligned/rotated between > 0° and 45°, and eight valves measured +2 on our scale, i.e., aligned/rotated between 45° and 90°. Twenty-three heart valve prostheses placed perpendicular to the magnetic field rotated by ≤ 45°, and 21 valves by between 45° and 90° (Table 2). This was true for mechanical, bioprosthetic, and human tissue valves.

DISCUSSION

MR imaging is used in an increasing number of patients. Each year, 150,000 heart valves are implanted worldwide (26). It is probable, therefore, that a number of patients with heart valve prostheses will be referred for an MR procedure. MR imaging is considered to be one of the safest non-invasive imaging modalities. However, anxieties persist amongst MR personnel about the potential dangers of performing a MR procedure on a patient with a biomedical implant or device. Such concerns relate to the possibility of a harmful interaction, namely translational and rotational forces, between the magnetic field and the implanted device (1–8). Yet, despite such apprehension, many implantable devices, including heart valves, are considered safe when implanted in a patient about to undergo a MR procedure when the static magnetic fields are 1.5 T or less (10,14,15,18,23,24,27–30). However, with the development of new systems with higher field strengths, it is possible that implants found to be diamagnetic or weakly ferromagnetic at field strengths of 1.5 T or less will be subjected to sufficiently large translational or rotational forces to present a potential hazard to the patient in these systems. Comparison of these results with those of a previous study using some of the same valves exposed to a 1.5-T MR system show a substantial increase in the translational forces, raising the possibility that further increases in field strength may indeed pose a threat to patient safety (24).

Translational attraction of a component is dependent upon the amplitude of the static magnetic field and its spatial gradient, as well as the object's dimensions, mass and orientation, its magnetic susceptibility, and the amount of fibrosing tissue securing the implant in place. In this study of 60 heart valves, the translational force gave rise to deflections that ranged from 0° to 7.5°. Only five valves did not deflect from the perpendicular. Although the alloys used in the heart valves tested, i.e., titanium, stellite, elgiloy, pyrolitic carbon, etc., are intrinsically non-magnetic and have been recommended alloys to use in the manufacture of biomedical implants (1), significant magnetic properties can be induced in such alloys by bending or cutting them, which may explain the deflections observed even with the porcine valves.

Forces acting on the object to rotate or align it parallel to the magnetic field depend on B_o^2, the object's dimensions, and its angle relative to the static magnetic field. Qualitative measures of torque in our study ranged from 0 to +2, and most valves displayed some alignment or rotation parallel to the magnetic field. However, it is not anticipated that these rotational forces will present a hazard or risk to the patient because none of the valves aligned with the magnetic field with any substantial torque; they only drifted into alignment.

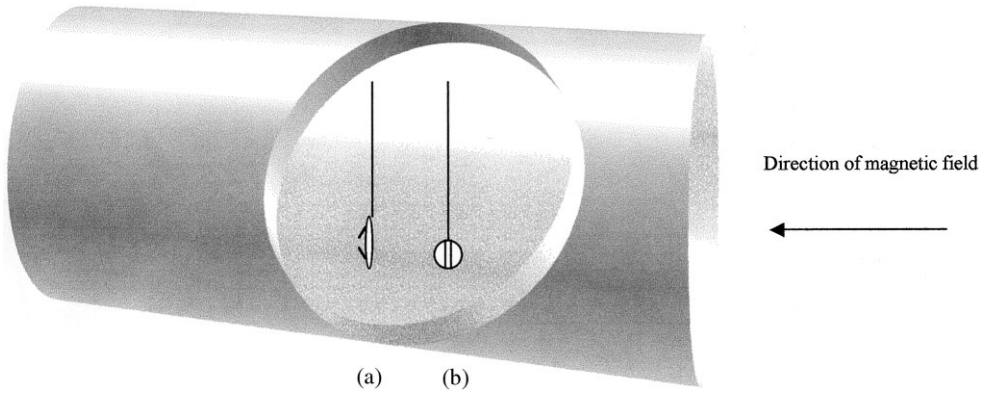

Figure 2. Diagram showing orientation of heart valve prosthesis measuring rotational forces in a 4.7-T MR system (side view) (a) The valve annulus is parallel to the magnetic field. (b) The valve annulus is perpendicular to the magnetic field.

Table 2
Magnetic Forces Acting on 60 Heart Valves at 4.7 T

No.	Valve	Site	Size (mm)	Deflection (degrees)	Torque (Parallel)[a]	Torque (Perpendicular)[b]	Magnetic moment (Am^2)	Magnetic force (N)	Force beating heart (N)
1	ATS Medical	Mitral	25	1	0	0	133×10^{-6}	6.6×10^{-3}	4.4–6.9
2	Beall	Mitral	29	2	2	2	1026×10^{-6}	5.1×10^{-3}	5.9–9.2
3	Biocor	Aortic	23	0	1	0	0	0	2.9–3.5
4	Bjork Shiley 60°cc	Aortic	27	5	1	1	692×10^{-6}	3.5×10^{-3}	4.0–4.9
5	Bjork Shiley 60°cc Valve Graft	Aortic	25	4	2	2	1011×10^{-6}	5.0×10^{-3}	4.6–5.6
6	Bjork Shiley Conical Disc	Mitral	21	3	0	0	454×10^{-6}	2.2×10^{-3}	3.1–4.8
7	Bjork Shiley Conical Disc	Mitral	21	3.5	1	1	486×10^{-6}	2.4×10^{-3}	3.1–4.8
8	Bjork Shiley Spherical Disc	Mitral	31	3.5	1	1	871×10^{-6}	4.4×10^{-3}	6.8–10.6
9	Bjork Shiley Monostrut	Aortic	17	4	1	1	482×10^{-6}	2.4×10^{-3}	1.6–1.9
10	Bjork Shiley Monostrut	Mitral	25	5	2	2	755×10^{-6}	3.8×10^{-3}	4.4–6.9
11	Bjork Shiley Monostrut	Mitral	23	5	1	1	980×10^{-6}	4.9×10^{-3}	3.7–5.8
12	Bjork Shiley Monostrut	Mitral	33	4	0	2	1359×10^{-6}	6.8×10^{-3}	7.7–12.0
13	Carbomedics	Aortic	21	0	1	1	0	0	2.4–2.9
14	Carbomedics	Aortic	23	0.5	1	1	50×10^{-6}	2.5×10^{-4}	2.9–3.5
15	Carbomedics	Mitral	31	0.5	2	2	102×10^{-6}	5.1×10^{-4}	6.8–10.6
16	Carbomedics	Mitral	29	0.5	0	2	92×10^{-6}	4.6×10^{-4}	5.9–9.2
17	Carbomedics Valve Graft	Aortic	34	–	2	2	–	–	6.4–7.7
18	Carpentier Edwards	Aortic	31	3	0	0	642×10^{-6}	3.2×10^{-3}	5.3–6.4
19	Carpentier Edwards Pericardial	Mitral	33	7	1	1	1508×10^{-6}	7.5×10^{-3}	7.7–12.0
20	Carpentier Edwards Supra-annular	Mitral	31	2.5	2	0	634×10^{-6}	3.2×10^{-3}	6.8–10.6
21	Durafic	Aortic	33	6[c]	0	2	611×10^{-6}	3.1×10^{-3}	6.0–7.3
22	Durafic	Mitral	23	2[c]	0	1	279×10^{-6}	1.4×10^{-3}	5.0–7.7
23	Duromedics	Aortic	27	0.5	0	2	265×10^{-6}	1.3×10^{-3}	5.3–6.5
24	Duromedics	Mitral	29	1	0	1	87×10^{-6}	4.4×10^{-4}	5.9–9.2
25	Hancock Pericardial	Mitral	25	1	0	0	166×10^{-6}	8.3×10^{-4}	4.4–6.9
26	Hancock Modified Orifice	Aortic	21	1	2	0	139×10^{-6}	7.0×10^{-4}	2.4–2.9
27	Hancock Modified Orifice II	Aortic	25	1	0	0	174×10^{-6}	8.7×10^{-4}	3.4–4.2
28	Intact	Aortic	19	2	0	0	218×10^{-6}	1.1×10^{-3}	2.0–2.4
29	Intact	Mitral	25	2	0	1	41×10^{-6}	2.1×10^{-4}	4.4–6.9
30	Ionescu Shiley	Aortic	23	1.5	0	1	286×10^{-6}	1.4×10^{-3}	3.9–4.7
31	Jyros	Aortic	26	6.5[c]	0	2	1171×10^{-6}	5.9×10^{-3}	3.7–4.5
32	Jyros	Mitral	30	7.5[c]	0	2	1839×10^{-6}	9.3×10^{-3}	3.4–9.9
33	Labcor	Aortic	21	2	1	1	245×10^{-6}	1.2×10^{-3}	2.4–2.9
34	Labcor	Mitral	25	2.5	0	0	441×10^{-6}	2.2×10^{-3}	4.4–6.9
35	Liotta	Aortic	23	2	1	0	338×10^{-6}	1.7×10^{-4}	2.9–3.5
36	Medtronic	Aortic	23	1	1	2	98×10^{-6}	4.9×10^{-4}	2.9–3.5
37	Medtronic	Mitral	23	2	0	2	279×10^{-6}	1.4×10^{-3}	3.7–5.8
38	Medtronic	Mitral	29	1	0	2	191×10^{-6}	9.6×10^{-4}	5.9–9.2
39	Mira	Mitral	27	0	0	0	0	0	5.2–8.0
40	Mitroflow	Aortic	25	2	1	1	246×10^{-6}	1.2×10^{-3}	3.4–4.2
41	Mitroflow	Aortic	25	2	2	2	221×10^{-6}	1.1×10^{-3}	3.4–4.2
42	Mitroflow	Mitral	29	2	0	2	287×10^{-6}	1.4×10^{-3}	5.9–9.2
43	Mitroflow Synergy	Aortic	21	3	0	0	217×10^{-6}	1.1×10^{-3}	2.4–2.9
44	Mosaic	Aortic	29	2	2	1	634×10^{-6}	3.2×10^{-3}	4.6–5.6
45	Omniscience	Mitral	25	0	0	2	0	0	4.4–6.9
46	On-X	Aortic	19	3	0	0	327×10^{-6}	1.6×10^{-3}	2.0–2.4
47	On-X	Mitral	31–33	3	0	0	776×10^{-6}	3.9×10^{-3}	6.8–12.0
48	Smellof Cutter	Aortic	21	0	0	2	496×10^{-6}	2.5×10^{-3}	2.4–2.9
49	Sorin Pericarbon (stented)	Mitral	33	1.5	1	1	393×10^{-6}	2.0×10^{-3}	7.7–12.0
50	St Jude Mechanical	Aortic	21	3	0	2	264×10^{-6}	1.3×10^{-3}	2.4–2.9
51	St Jude Mechanical	Mitral	27	3.5	0	2	505×10^{-6}	2.5×10^{-3}	6.9–10.7
52	Starr Edwards	Mitral	32	0	0	0	0	0	7.2–11.3
53	Starr Edwards	Mitral	32	6.5[c]	0	0	2642×10^{-6}	13.2×10^{-3}	7.2–11.3
54	Starr Edwards	Mitral	26	4[c]	0	1	1008×10^{-6}	5.0×10^{-3}	6.4–9.9
55	Tascon	Aortic	23	6[c]	0	1	1813×10^{-6}	9.1×10^{-3}	3.9–4.7
56	Ultracor	Aortic	23	1	0	2	109×10^{-6}	5.5×10^{-4}	2.9–3.5
57	Ultracor	Mitral	25	1	0	1	134×10^{-6}	6.7×10^{-4}	4.4–6.9
58	Wessex	Aortic	31	2	1	1	494×10^{-6}	2.5×10^{-3}	5.3–6.4
59	Wessex	Mitral	25	2	0	1	379×10^{-6}	1.9×10^{-3}	4.4–6.9
60	Xenofic	Aortic	23	2	0	1	457×10^{-6}	2.3×10^{-3}	2.9–3.5

[a]Parallel to the magnetic field.
[b]Perpendicular to the magnetic field.
[c]These valves were attracted towards the centre of the magnet, all other valves deflected away from the center of the magnet.

An implant or device is considered unsafe to undergo a MR procedure if it is known to be ferromagnetic, and/or if ex vivo testing has identified it to deflect at an angle $\geq 45°$ (31) and if the magnetic force on the implant is a significant fraction of that applied in the normal in vivo application of the device (9–11). Table 2 shows that all the heart valves fell well within the current safety limits, and the resultant magnetic forces

exerted on each heart valve prosthesis was significantly smaller than the mechanical forces of the beating heart. Moreover, heart valves are secured by multiple sutures and become endothelialized after six weeks, serving to retain the prosthesis in place during exposure to the MR environment (9,29). Based on these criteria, all 60 heart valve prostheses listed in Table 1 would be considered safe to undergo a MR procedure at 4.7 T or less.

Although this study has not investigated the potential hazards of either time-varying gradient magnetic fields or the radiofrequency (RF) excitation fields at 4.7 T, the authors believe heating of components (1,9,12,32–33) due to the latter is not expected to be dependent on magnetic field strength, provided RF peak power requirements are not substantially increased. However, higher field strength magnets may require higher RF and gradient fields, and, therefore, the appropriate allowances must be made for increased potential RF heating.

Sixty heart valve prostheses were evaluated for MR safety by studying magnetic forces exerted on them within the bore of a 4.7-T system. Criteria previously used for safety assessment of biomedical implants and devices and expressed in terms of magnetic forces suggest that the forces observed in this study are all compatible with the safe use of these valves in MR systems with static fields up to 4.7 T.

ACKNOWLEDGMENTS

The authors would like to thank Professor Ian Young of the Magnetic Resonance Imaging Unit at the Hammersmith Hospital in London; Alasdair Hall, Senior Research Associate at the MRC, Hammersmith Hospital, London; and Drs. Pat Lawford and Rod Hose of the Department of Medical Physics and Engineering at the Hallamshire Hospital, Sheffield for their help and support throughout this study. The authors are also grateful to Medtronic Hall of Watford (UK), Sulzer Carbomedics of Crawley, West Sussex (UK), ATS Medical, Inc. of Minneapolis, MN (USA), and Pulse Surgical, Ltd. of Chinnor, Oxon (UK) who provided many of the valves for the study.

REFERENCES

1. New PFJ, Rosen BR, Brady TJ, et al. Potential hazards and artefacts of ferromagnetic and non-ferromagnetic surgical and dental devices in nuclear magnetic resonance imaging. Radiology 1983;147:139–148.
2. Yuh WTC, Hanigan MT, Nerad JA, et al. Extrusion of eye socket magnetic implant after MR imaging examination: potential hazard to patient with eye prosthesis. J Magn Reson Imaging 1991;1:711–713.
3. Klucznik R, Carrier D, Pyka R, Haid R. Placement of a ferromagnetic intracerebral aneurysm clip in a magnetic field with a fatal outcome. Radiology 1993;187:855–856.
4. Shellock FG, Crues JV. High-field MR imaging of metallic implants: an ex vivo evaluation of deflection forces. AJR Am J Roentgenol 1988;151:389–392.
5. Kanal E, Shellock FG, Lewin JS. Aneurysm clip testing for ferromagnetic properties: clip variability issues. Radiology 1996;200:576–578.
6. Bromage PR, Kozic Z. Magnetic resonance imaging implications of metal-reinforced spinal microcatheters. J Clin Anesth 1991;3:382–385.
7. Malt JC. Hazards of ferrous materials in MRI: a case report. Radiol Technol 1997;53:233–235.
8. Boutin RD, Briggs JE, Williamson MR. Injuries associated with MR imaging: survey of safety records and methods used to screen patients for metallic foreign bodies before imaging. AJR Am J Roentgenol 1994;162:189–194.
9. Shellock FG, Kanal E. Magnetic resonance: bioeffects, safety, and patient management. New York: Lippincott, Williams & Wilkins; 1996 p 127–170.
10. Shellock FG. Pocket guide to MR procedures and metallic implants: update 2000. Philadelphia: Lippincott, Williams & Wilkins; 2000.
11. Sawyer-Glover AM, Shellock FG. Pre-MRI procedure screening: recommendations and safety considerations for biomedical implants and devices. J Magn Reson Imaging 2000;12:92–106.
12. Kanal E, Shellock FG, Talagala L. Safety considerations in MR imaging. Radiology 1990;175:593–606.
13. Hathout G, Lufkin RB, Jabour B, et al. MR-guided aspiration cytology in the head and neck at high field strength. J Magn Reson Imaging 1992;2:93–94.
14. Kotaskis A, Tan KH, Jackson G. Is MRI a safe procedure in patients with coronary stents in situ? Int J Clin Pract 1997;51:349.
15. Pride GL, Kowal J, Mendelsohn DB, et al. Safety of MR scanning in patients with nonferromagnetic aneurysm clips. J Magn Reson Imaging 2000;12:198–200.
16. Hasenkam JM, Ringgaard S, Houlind K, et al. Prosthetic heart valve evaluation by magnetic resonance imaging. Eur J Cardiothorac Surg 1999;16:300–305.
17. High WB, Sikora J, Ugurbil K Garwood M. Subchronic in vivo effects of a high static magnetic field (9.4 T) in rats. J Magn Reson Imaging 2000;12:122–139.
18. Kangarlu A, Shellock FG. Aneurysm clips: evaluation of magnetic field interactions with an 8.0 T MR system. J Magn Reson Imaging 2000;12:107–111.
19. Magin RL, Lee JK, Klintsova A, et al. Biological effects of long-duration, high-field (4 T) MRI on growth and development in the mouse. J Magn Reson Imaging 2000;12:140–149.
20. Williams MD, Antonelli PJ, Williams LS, Moorhead JE. Middle ear prosthesis displacement in high-strength magnetic fields. Otol Neurotol 2001;22:158–161.
21. Condon B, Hadley DM. Potential MR hazard to patients with metallic heart valves: the Lenz effect. J Magn Reson Imaging 2000;12:171–176.
22. Robertson NM, Diaz-Gomez M, Condon B. Estimation of torque on mechanical heart valves due to magnetic resonance imaging including an estimation of the significance of the Lenz effect using a computational model. Phys Med Biol 2000;45:3793–3807.
23. Edwards MB. 25 years of heart valve replacements in the United Kingdom. A guide to types, models and MRI safety. London: UK Heart Valve Registry; 2000.
24. Edwards MB, Taylor KM, Shellock FG. Prosthetic heart valves: evaluation of magnetic field interactions, heating, and artifacts at 1.5 T. J Magn Reson Imaging 2000;12:363–369.
25. Schenck JF. Safety of strong, static magnetic fields. J Magn Reson Imaging 2000;12:2–19.
26. Edwards MB, Taylor KM. A profile of valve replacement surgery in the UK (1986–1997): a study from the UK Heart Valve Registry. J Heart Valve Dis 1999;8:697–701.
27. Randall PA, Kohman LJ, Scalzetti EM, et al. Magnetic resonance imaging of prosthetic cardiac valves in vitro and in vivo. Am J Cardiol 1988;62:973–976.
28. Hassler M, Le Bas JF, Wolf JE, et al. Effects of magnetic fields used in MRI on 15 prosthetic heart valves. J Radiol 1986;67:661–666.
29. Soulen RL, Budinger TF, Higgins C. Magnetic resonance imaging of prosthetic heart valves. Radiology 1985;154:705–707.
30. Pruefer D, Kalden P, Schreiber W, et al. In vitro investigation of prosthetic heart valves in magnetic resonance imaging: evaluation of potential hazards. J Heart Valve Dis 2001;10:410–414.
31. American Society for Testing and Materials. Standard specification for the requirements and disclosure of self-closing aneurysm clips. ASTM Designation Standard F1542-94:1–3. Pennsylvania: ASTM International; 2000.
32. Buchli Boesiger P, Meier D. Heating effects of metallic implants by MRI examinations. Magn Reson Med 1988;7:255–261.
33. Davis PL, Crooks L, Arakawa M, et al. Potential hazards in NMR imaging: heating effects of changing magnetic fields and RF fields on small metallic implants. AJR Am J Roentgenol 1991;173:857–860.